ACS APPLIED MATERIALS & INTERFACES

Research Article

www.acsami.org

Monodisperse Hollow Silica Nanospheres for Nano Insulation Materials: Synthesis, Characterization, and Life Cycle Assessment

Tao Gao,*[,†] Bjørn Petter Jelle,[‡,§] Linn Ingunn C. Sandberg,[‡] and Arild Gustavsen[†]

[†]Department of Architectural Design, History and Technology and [‡]Department of Civil and Transport Engineering, Norwegian University of Science and Technology (NTNU), NO-7491 Trondheim, Norway

[§]Department of Materials and Structures, SINTEF Building and Infrastructure, NO-7465 Trondheim, Norway

ABSTRACT: The application of manufactured nanomaterials provides not only advantages resulting from their unique properties but also disadvantages derived from the high energy use and CO_2 burden related to their manufacture, operation, and disposal. It is therefore important to understand the trade-offs of process economics of nanomaterial production and their associated environmental footprints in order to strengthen the existing advantages while counteracting disadvantages. This work reports the synthesis, characterization, and life cycle assessment (LCA) of a new type of superinsulating materials, nano insulation materials (NIMs), which are made of hollow silica nanospheres (HSNSs) and have great flexibility in modifying their properties by tuning the corresponding structural parameters. The as-prepared HSNSs in this work have a typical inner pore diameter of about 150 nm and a shell thickness of about 10−15 nm and exhibit a reduced thermal conductivity of about 0.02 W/(m K) because of their size-dependent thermal conduction at the nanometer scale. The energy and raw material consumption related to the synthesis of HSNSs have been analyzed by the LCA method. The results indicate that the recycle of chemicals, up-scaling production, and use of environmentally friendly materials can greatly affect the process of environmental footprints. New synthesis routes for NIMs with improved thermal performance and energy and environmental features are also recommended on the basis of the LCA study.

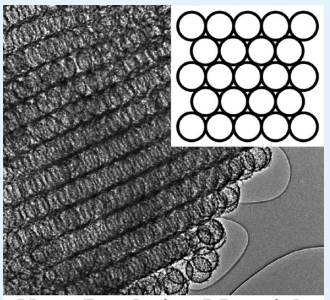

KEYWORDS: *hollow silica nanospheres, nano insulation materials, thermal insulation, life cycle assessment, embodied energy, environmental footprint*

1. INTRODUCTION

The past couple of decades have witnessed an exponential growth of research and development activities in nanotechnology, which has been making a ground-breaking impact on various science, engineering, and commercial sectors.[1,2] Although the application of nanotechnology in biomedical and electronic industries is still of priority to some extent,[1,2] the construction industry has recently started seeking out a way to advance conventional building materials/components by using a variety of nanomaterials.[3−5] It has been revealed that the application of nanotechnology can improve vital characteristics of building materials, such as strength and durability, and endow them with new and useful properties.[3−5] Silica aerogels, for example, are a nanoporous translucent material with very low density and low thermal conductivity compared to other known solids.[6,7] The unique properties of silica aerogels make them an ideal multifunctional material for various applications,[8] for example, as thermal insulation materials[9] and window glazing[10] in the building sector. However, silica aerogels are very brittle and costly, which hinder their practical applications in many areas.[11] Many research efforts have therefore been carried out to enhance the mechanical properties of silica aerogels[12−14] and also to reduce their manufacturing costs.[15,16]

The promising future of silica aerogels also inspires research dedicated to new nanomaterials or nanostructures that have similar or better properties compared to silica aerogels.[17−21] Carbon nanotube aerogels[19] and graphene aerogels,[20,21] for example, have recently been developed and exhibit novel structural and electrical properties, offering possibilities for various applications. Another example is nano insulation materials (NIMs),[22] which can be assembled by using hollow silica nanospheres (HSNSs) with dimensions of about 100 nm and exhibit a reduced thermal conductivity of about 0.02 W/(m K),[23−25] comparable to that of silica aerogel granules.[11] One distinctive advantage of HSNS NIMs for thermal insulation application is their controllability; i.e., by modification of the particle size and porosity, their thermal and/or other properties can be controlled over a large range.[23] Nevertheless, it must be pointed out that turning the conceptual HSNS NIMs into practical thermal insulation materials may require substantial research efforts dedicated to this field.

Nowadays, it is generally accepted that any new materials or technologies shall be developed in accordance with the principles of sustainable development.[26] The application of nanomaterials provides obvious advantages thanks to their unique properties. On the other hand, disadvantages may be derived from the high energy use and CO_2 burden related to the manufacture, operation, and disposal of nanomaterials.[27,28]

Received: October 12, 2012
Accepted: January 18, 2013
Published: January 18, 2013

It is therefore critical to understand the trade-offs of process economics with their associated environmental footprints in order to build on existing strengths while counteracting disadvantages. Life cycle assessment (LCA) represents a comprehensive framework that quantifies ecological and human health impacts of a product or system over its complete life cycle.[29] Not surprisingly, research applying the LCA approach to the area of nanomaterials and nanotechnology is of great interest.[29−40] Literature covering silica aerogels,[30] carbon nanotubes,[31−33] carbon nanofibers,[34,35] silver nanoparticles,[36] and several nanoenabled products[37−40] has so far been reported. However, it must be pointed out that there are still many issues that need further precision for application of the LCA approach in the field of nanotechnology.[29] Moreover, application of the LCA approach for other nanomaterials, especially the newly developed nanomaterials with specific functions, is scarce.

It is obviously interesting and important to apply the LCA approach to the development of HSNS NIMs. This is of particular importance at the early stage of development because many different synthetic approaches with different energy and environment features can be employed,[23−25] which will affect the ecological impacts of the final NIMs. In this work, we report the synthesis and characterization of HSNSs with reduced thermal conductivities, which may be used to assemble NIMs for various applications. A "cradle-to-factory gate" LCA approach[30] is conducted and reveals the importance of the recycle of chemicals, up-scaling production, and use of environmentally friendly materials to improve both the thermal performance and energy features of HSNSs. On the basis of the LCA results, new synthetic routes for HSNSs for NIM applications are recommended. The methodology reported here can also be extended to other nanomaterials, where the concern for their energy and environmental impact is of high priority.

2. SYNTHESIS OF HSNS

2.1. Materials and Chemicals. Reagent-grade styrene (99%), poly(vinylpyrrolidone) (PVP; $M_w \approx 40000$), potassium persulfate (KPS; 99%), tetraethyl orthosilicate (TEOS; 98%), ethanol (96%), and ammonium hydroxide (NH_4OH; 28−30% NH_3 basis) were purchased from Sigma-Aldrich and used without further purification.

2.2. Synthesis of Polystyrene (PS) Nanospheres. Monodisperse PS nanospheres were first prepared and served thereafter as templates for the growth of silica coatings. For a typical synthesis, 1.5 g of PVP was dissolved in 100 mL of distilled water under ultrasonic irradiation, and to this solution was added 10 g of a styrene solution. The obtained styrene/PVP solution was then heated to 70 °C under constant stirring at 500 rpm. Afterward, 10 mL of a KPS solution (0.15 g of KPS in 10 mL of water) was added dropwise into the PVP/styrene solution to initiate the polymerization reaction. The polymerization reaction was kept at 70 °C for 24 h. After the reaction, the obtained PS nanosphere suspension was cooled naturally to room temperature for further use.

2.3. Coating of the PS Nanospheres with Silica. For a typical synthesis, 6 g of an as-prepared PS suspension and 4 mL of a NH_4OH solution were added into 120 mL of ethanol under constant stirring at 500 rpm. Then, 10 mL of a TEOS/ethanol solution (50 vol % TEOS in ethanol) was slowly added. The reaction system was stirred for 10−24 h to prepare core−shell-type PS@SiO_2 nanospheres. After the reaction, the solid product was separated from the mother solution by centrifugation. The obtained sediment was washed with ethanol two times and finally dried at room temperature. HSNSs were readily obtained by annealing the PS@SiO_2 nanospheres at 500 °C in air for 3 h.

2.4. Characterization. Transmission electron microscopy (TEM; JEM-2010) was employed to characterize the morphology and microstructure of the as-synthesized products. Thermal conductivity of the obtained materials was analyzed by using a Hotdisk Thermal Constants Analyzer (TPS 2500S). A disk-type Kapton Sensor 5464 with a radius of 3.189 mm was used. The sensor, which acts as both a heat source and a temperature recorder, was sandwiched in two parts of the powdered samples. The temperature increase of the samples as a function of time was recorded to compute the thermal conductivity (uncertainty: ∼5%). The final thermal conductivity value reported here was the arithmetic mean of four individual measurements under different conditions (heating power, 0.02−0.200 W; measurement time, 1−160 s).

3. LCA OF HSNS

3.1. Methodology. A "cradle-to-factory gate" LCA approach was considered by following a published procedure[30] with modifications. Primary data were collected from the synthesis of HSNSs, as mentioned above. Secondary data were used to account for the energy use from the extraction of raw materials as well as the grid intensity of electricity. Figure 1 outlines the system boundary for this LCA study. Note that some parameters were not considered because of the lack of source data of relevant chemicals/processes. Therefore, it should be treated with caution when applying for other synthetic processes or materials.

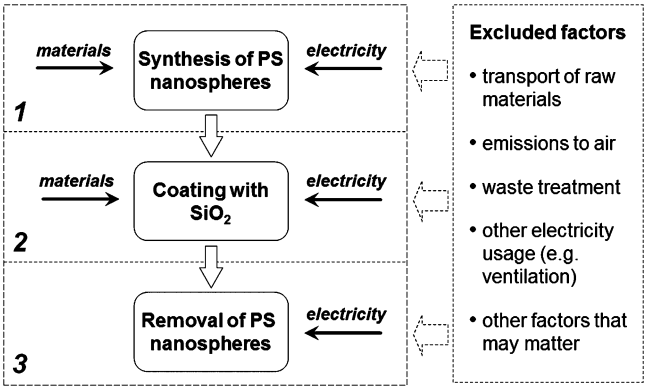

Figure 1. System boundary for LCA of HSNSs from the PS nanosphere templating method. There are three main steps (1−3) in the material preparation.

3.2. Data Collection. The material and energy consumption data during the synthesis are summarized in Tables 1 and 2, respectively. About 1.05 g of HSNSs was obtained as the final product at these experimental conditions.

4. RESULTS AND DISCUSSION

Synthesis and Structural Features of HSNSs. A hollow or porous structure that takes the advantages of air cavities with low thermal conductivity [about 0.026 W/(m K) at ambient condition][41] is important to obtain thermal insulation materials. For superinsulating materials or NIMs with thermal conductivities lower than air at standard temperature and pressure

Table 1. Material Consumption for the Synthesis of HSNSs

raw materials	volume (mL)	mass (g)	material supplier
Step1: Synthesis of PS Nanospheres			
H_2O	110	110	in-house
styrene		10	Sigma-Aldrich
PVP		1.5	Sigma-Aldrich
KPS		0.1	Sigma-Aldrich
Step 2: Coating of PS Nanospheres with Silica			
ethanol	206[a]	162	Sigma-Aldrich
PS[b]		6	from above
NH_4OH	4		Sigma-Aldrich
TEOS	5		Sigma-Aldrich

[a]Including also the ethanol used for washing the particles. [b]PS nanosphere suspension.

Table 2. Electricity Consumption for the Synthesis of HSNSs[a]

equipment	running time (h)	total energy (kWh)	equipment supplier
Step 1: Synthesis of PS Nanospheres			
IKA hot-plate magnetic stirrer (heating on)	20	0.95	Sigma-Aldrich
Step 2: Coating of PS Nanospheres with Silica			
IKA hot-plate magnetic stirrer (heating off)	5	0.03	Sigma-Aldrich
Allegra X-22 centrifuge	1	0.15	Backman
Step 3: Removal of the PS Nanosphere Template			
Carbolite furnace	3	0.58	Sigma Aldrich

[a]The electricity consumption is recorded with an energy and power meter.

(STP) condition, nanoporous materials are usually considered, which take the advantage of size-dependent thermal conduction presented typically at the nanometer scale.[42,43] The methodology of achieving NIMs by using hollow nanospheres is depicted in Figure 2. The overall property of the hollow

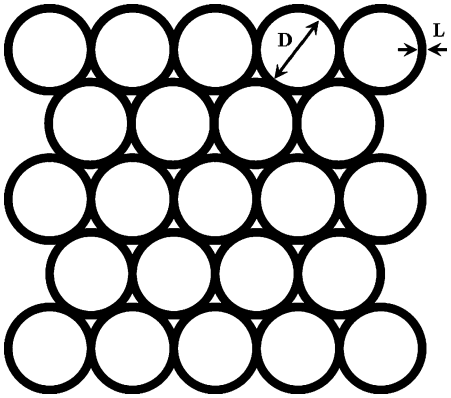

Figure 2. Schematic drawing of the hollow nanosphere NIMs. *D* and *L* represent the pore diameter and shell thickness of the hollow nanospheres.

nanosphere NIMs depends on several parameters, such as the diameter and shell thickness of the hollow spheres, the chemical composition of the shell materials, the type of filled gas, and the packing manner or density of these hollow spheres.[23] Therefore, through modification of these structural or compositional parameters, the thermal performance of the hollow nanosphere NIMs can be readily controlled over a large range.

Silica represents probably one of the best candidate materials for achieving hollow nanosphere NIMs because of the fact that silica is abundant in nature and also environmentally friendly. HSNSs have so far been extensively studied because of their well-defined structural features, novel physical and chemical properties, and important applications in various sectors.[44−46] As shown in Figure 2, the presence of a large fraction of air cavities within the nanometer range can greatly suppress thermal conduction through the HSNSs, making them an ideal system for achieving superinsulating materials or NIMs.[23]

HSNSs can be prepared via many different methods, such as a template-assisted method[47] or a dissolution−recrystallization growth process.[48−50] Among these, the template-assisted approach represents probably the most straightforward method and has many distinctive advantages.[51] As shown schematically in Figure 3, the template, which provides the nucleation sites

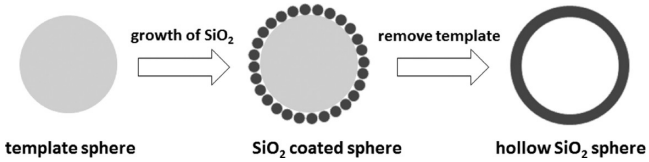

Figure 3. Schematic drawing of the template-assisted approach for HSNSs.

for the subsequent growth of silica, can, in principle, be any materials with a desirable morphology, such as gaseous bubbles,[24] liquid droplets,[52,45] or solid particles.[23,25,53−57] In this work, PS nanospheres were selected as a template material for the growth of HSNSs because of the fact that monodisperse PS nanospheres can be readily prepared with controlled diameters and surface properties;[53−57] in addition, as a sacrificed template, PS nanospheres can be conveniently removed by heating or dissolution.[55−57]

Figure 4 shows the TEM images of the as-prepared PS nanospheres in this work. Under the present experimental

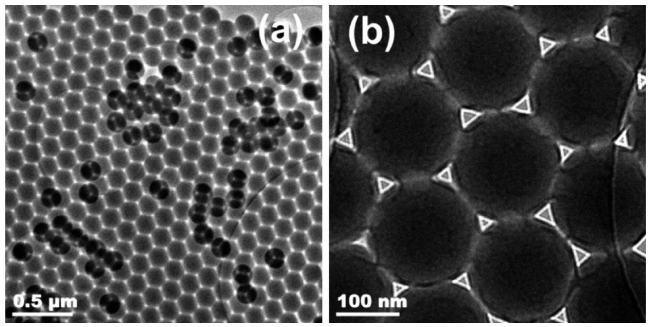

Figure 4. TEM images of the as-synthesized PS nanospheres with a mean diameter of about 150 nm.

conditions, the as-synthesized monodisperse PS nanospheres have a mean diameter of about 150 nm. It is worth pointing out that the size of the PS nanospheres can be controlled by changing, e.g., the amount of PVP used in the synthesis.[54] Large PS nanospheres with diameters of about 900 nm can be obtained when the PVP/styrene weight ratio is about 0.005, whereas increasing the PVP/styrene ratio to about 0.05 results in PS nanospheres with smaller diameters of about 280 nm. In

this work, the 150-nm PS nanospheres were prepared with a PVP/styrene ratio of 0.15. Thanks to their relatively small sizes and corresponding large surface-to-volume ratio, the surface of PS nanospheres is very active, thus providing an ideal nucleation site for the subsequent growth of silica.

Hydrolysis of TEOS in a basic environment results in the formation of silica nanoparticles, of which the particle size depends on several experimental parameters such as the water/ethanol ratio, the concentrations of NH_4OH and TEOS, and also the reaction temperature.[58] With the presence of presynthesized PS nanospheres, silica molecules produced from the hydrolysis of TEOS will be captured by and deposit at the surface of the PS nanospheres. It is obvious that a positively charged surface of PS nanospheres may help to catch the primary silica particles that are known to be negatively charged.[53−57]

Figure 5 shows TEM images of the as-synthesized HSNSs in this work. The hollow spheres exhibit typical shell thicknesses

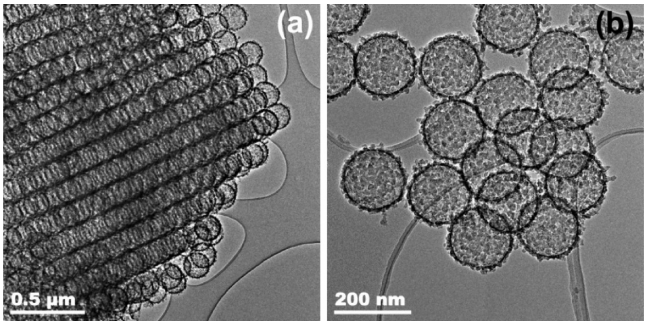

Figure 5. TEM images of the as-synthesized HSNSs.

of 10−15 nm and pore diameters of about 150 nm. Hence, the inner diameter of the as-prepared HSNSs agrees well with that of the PS nanosphere templates (see Figure 4), indicating the advantage of this template-assisted approach for the synthesis of monodisperse hollow nanostructures. Note that the shell of HSNSs consists of silica nanoparticles with typical sizes of about 5−10 nm, indicating that the primary silica particles produced from hydrolysis of TEOS aggregate together and form secondary particles before they deposit on the surface of the PS templates. This is because the surface of the PS nanospheres used here is negatively charged, which repulses the silica nanoparticles with the same negative surface charges.[54]

By using PS nanosphere templates with different sizes and by controlling the hydrolysis reaction of TEOS, HSNSs with different structural features can be prepared, as shown in Figure 6a. Moreover, by modifying the surface of the PS nanospheres, e.g., using PS nanospheres with positively charged surfaces,[55−57] HSNSs with rather smooth surfaces can also be obtained (Figure 6b). However, it is worth pointing out that, for achieving NIMs with low thermal conductivities, a rough surface of the as-prepared HSNSs (i.e., Figure 5) represents actually a desirable feature because it can increase the phonon scattering and thereby suppress further the solid thermal conduction.[42,43,59] Moreover, a small pore size (e.g., inner diameter <200 nm) is also preferred in order to achieve suppressed gaseous thermal conduction. A more detailed discussion can be found in the following section.

Thermal Properties of HSNSs. The thermal properties of the as-synthesized HSNSs were characterized by using a transient plane source technique.[60] Figure 7 reports the

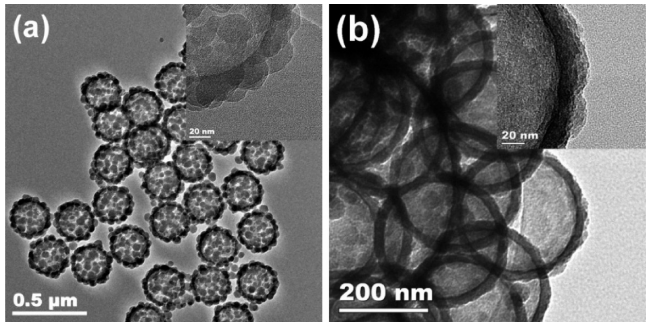

Figure 6. TEM images of two additional HSNS samples with different diameters and shell structures. The samples were prepared by using different PS nanosphere templates and under slightly different experimental conditions. (a) HSNSs with a mean diameter of about 200 nm and a shell thickness of about 25 nm. (b) HSNSs with a smooth surface compared to the HSNS samples shown in panel a. Insets in panels a and b are the high-magnification TEM pictures, showing details of the shell structure.

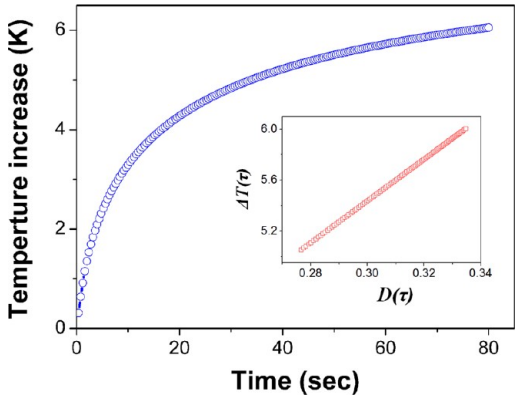

Figure 7. Transient graph of the as-prepared HSNSs. The inset shows a computational plot of the temperature increase $\Delta T(\tau)$ versus $D(\tau)$. The definition of the terms is given in the text.

transient graph of HSNSs, where the time-dependent temperature increase $\Delta T(\tau)$ is given by[60]

$$\Delta T(\tau) = \frac{P_o}{\pi^{3/2}\alpha\lambda} D(\tau) \quad (1)$$

where P_o is the total output of power from the sensor, α is the overall radius of the disk spiral (α = 3.189 mm in this work), λ is the thermal conductivity of the HSNS sample, and $D(\tau)$ is a dimensionless time-dependent function with

$$\tau = \sqrt{\frac{t}{\theta}} \quad (2)$$

where t is the time measured from the start of the transient recording and θ is the characteristic time defined as

$$\theta = \frac{\alpha^2}{\kappa} \quad (3)$$

where κ is the thermal diffusivity of the HSNS sample. When a computational plot is made of the recorded temperature increase $\Delta T(\tau)$ versus $D(\tau)$, a straight line can be obtained, with the slope being $P_o/\pi^{3/2}\alpha\lambda$ (inset of Figure 7). By knowing the heating power P_o and the radius of the disk spiral α, the thermal conductivity λ can be calculated. In this work, the as-prepared HSNSs (i.e., Figure 5) have an effective thermal

dx.doi.org/10.1021/am302303b | ACS Appl. Mater. Interfaces 2013, 5, 761−767

conductivity of 0.020 ± 0.002 W/(m K), similar to that of the silica aerogel granules.[11]

The low thermal conductivity of HSNSs, ~0.02 W/(m K), compared to the bulk value of 1.4 W/(m K) for silica,[41] can be interpreted by the size-dependent thermal conduction appearing typically at the nanometer scale.[42,43] For example, the size-dependent gaseous thermal conductivity (λ_g) can be understood by the Knudsen effect, which considers gaseous thermal transport in a space with small dimensions:[22]

$$\lambda_g = \frac{\lambda_{g,0}}{1 + 2\beta Kn} \quad (4)$$

where $\lambda_{g,0}$ is the thermal conductivity of gas at STP, β is a constant depending on the type of gas (for air, $\beta \approx 1.5-2$), $Kn = l/d$ is the Knudsen number, with l being the gas molecule mean-free path (for air, $l \approx 68$ nm at ambient condition)[41] and d being the dimension where the gaseous transport takes place, e.g., the inner pore diameters of HSNSs (Figure 2). It is evident that, for pores with diameters of a few nanometers, the Knudsen number becomes very large, resulting eventually in $\lambda_g \rightarrow 0$. In this work, the as-prepared HSNSs have a pore diameter of about 150 nm, which brings about a theoretical gaseous thermal conductivity of about 0.010 W/(m K) according to eq 4.

Other contributions from, e.g., solid thermal conduction and thermal radiation,[23] shall also be taken into account to understand the measured thermal conductivity of HSNSs, 0.02 W/(m K). For solid materials, there exists a prominent size-dependent thermal conductivity when their characteristic dimensions are not significantly greater than the mean free path of phonons or electrons, i.e., typically at the nanometer scale.[42,43] Liang and Li have proposed a phenomenological theory for the size-dependent thermal conductivity of nanoscale semiconductor systems.[59] Accordingly, the thermal conductivity of solid nanospheres λ_N can be expressed as[59]

$$\frac{\lambda_N}{\lambda_B} = p \exp\left(-\frac{l_0}{D}\right)\left[\exp\left(\frac{1-\alpha}{D/D_0 - 1}\right)\right]^{3/2} \quad (5)$$

where λ_B is the thermal conductivity of the bulk material, l_0 is the phonon mean free path at room temperature, D is the diameter of the nanospheres (in this work, it corresponds to the shell thickness of the HSNS, L; Figure 2), D_0 and α are material-dependent constants, and p is a factor reflecting the surface roughness, $0 \le p \le 1$, where $p \rightarrow 1$ corresponds to a smooth surface with a greater probability of specular phonon scattering and $p \rightarrow 0$ corresponds to a rough surface with a greater probability of diffusive phonon scattering.[61,62] It is therefore reasonable that the HSNSs with rough surfaces (i.e., Figures 5 or 6a) or small p values will, in general, have lower solid thermal conductivities. This explains the relatively low thermal conductivity [~0.024 W/(m K)] of the HSNS sample shown in Figure 6a compared to that of the HSNS sample shown in Figure 6b [~0.028 W/(m K)], within the experimental error range. Moreover, according to eq 5, one can conclude that a thin shell thickness (i.e., a small value of L; see Figure 2) of HSNSs will result in a lower solid thermal conductivity than that with a thick shell thickness or large L value. Although the detailed calculation for HSNSs based on eq 5 is difficult at this stage because of the lack of material-dependent parameters, the contribution from the solid thermal conductivity is, in general, small[25] because of the existence of a "neck area" (contact area) with typical sizes of a few nanometers between adjacent spheres.[63]

It is also important to point out that the as-prepared HSNSs in this work are hydrophilic, which is different from the silica aerogel granules, which are usually hydrophobic.[11] The hydrophilic nature, small size, and large surface area of HSNSs may result in a certain amount of water absorption, which contributes also to the measured thermal conductivity of HSNSs because of the relatively high thermal conductivity of water [$\lambda \approx 0.6$ W/(m K)].[41] However, it is difficult to measure/calculate the contribution from water absorption. By modification of the surface of the as-prepared HSNSs, it is possible to obtain the hydrophobic counterparts with different or probably better thermal performance than the hydrophilic ones. New syntheses along this direction are underway.

LCA and Data Interpretation of HSNSs. Table 3 reports the production impact associated with making 1 g HSNSs. The calculated production energy (or embodied energy) for the as-prepared HSNSs is about 2.65 MJ/g, which seems very high even compared to that of the energy-intensive thermal insulation materials, PS, about 0.105 MJ/g.[64] However, it is understandable because this work is a laboratory test and is also in a small scale. For example, a previous study on silica aerogels also resulted in quite high values for the embodied energy, i.e., about 7.3 MJ/g, for silica aerogels obtained from a high-temperature supercritical drying process.[30]

Table 3. Production Impact Associated with Making 1 g HSNSs

		embodied energy (MJ/kg)	amount (g)	production energy (MJ/g)
materials	PS	105[64]	0.5[a]	0.053
	ethanol	15.7[65]	162	2.54
	NH_4OH	43.15[66]	1.05[b]	0.045
	TEOS		4.76[c]	
electricity		10.5 MJ/kWh[66]	0.81 kWh[a,d]	0.009
total				2.65

[a]Assuming that 10 g of styrene converts totally into PS; only part of the PS suspension is used for the one synthesis of HSNSs. [b]The weight of NH_3. [c]The value correlates also with the purity of TEOS, 98%. [d]Part of the electricity from step 1 adds to those consumed in steps 2 and 3 (see Table 2).

It must be pointed out that the uncertainty of the obtained value, 2.65 MJ/g for HSNSs in this work, is probably large because some parameters that affect the calculation are not considered, such as the energy factor of TEOS (see also Figure 1). Therefore, the LCA method and the conclusions reported here should be treated with caution when applied for other synthetic approaches or materials. A data interpretation of this LCA study (Table 3) is given below to understand the process economics and environmental footprints of HSNSs.

Upscaling the synthesis will reduce the embodied energy of HSNSs. A parallel study indicates that the present experimental condition (Tables 1 and 2) can be readily adapted (e.g., by increasing the PS dosage) to the synthesis of ~2 g HSNSs, and a reduced embodied energy value of about 1.4 MJ/g has been obtained. Obviously, a large-scale synthesis, where the raw materials and electricity can be used more efficiently, is important to reduce the embodied energy of HSNSs.

Recycling of chemicals such as ethanol is important to reduce the embodied energy of HSNSs. In this work, the use of

ethanol represents the most energy-intensive step in the whole process (Table 3). This is due to the relatively large quantity of ethanol needed for a controlled hydrolysis of TEOS. Recycling of ethanol will change dramatically the energy feature of HSNSs. For example, an 80% recycling of ethanol during the production may reduce the embodied energy of HSNSs from 2.65 to ~0.62 MJ/g. Recycling of other chemicals, especially the energy-intensive PS,[64] is also important.

The use of environmentally friendly templating materials during the synthesis should be considered. In this work, as a sacrificed template, PS nanospheres need to be removed to obtain the final product. However, PS has a high embodied energy, about 105 MJ/kg.[64] Note that all of the embodied energy of PS nanospheres will be transferred to HSNSs if the PS nanosphere templates are burnt away (Figure 3 and Table 2), which will make HSNS a material with high embodied energy. Dissolving PS nanospheres by a certain chemical solvent[57] seems necessary from the viewpoint of recycling, though the recycling potential of the dissolved PS and the chemical solvent remains uncertain. An alternative in this regard might be the use of other templating materials with less environmental footprints and/or ease to recycle, such as $CaCO_3$ nanoparticles.[67,68] Moreover, Yue et al. reported previously the use of SiF_4 gas to produce HSNSs,[24] which may represent another possibility. However, some toxic/corrosive raw materials and byproducts involved in this synthetic method[24] must also be taken into account.

The use of other silica sources such as sodium silicate (i.e., water glass) with less environmental impact than that of TEOS is worth pursuing.[15] To the best of our knowledge, there are no data available at this stage for the embodied energy or emission factor of TEOS,[30] which explains the exclusion of TEOS from the LCA approach (Table 3) in this work. However, TEOS is likely an energy-intensive material because the production may involve some energy-intensive raw materials such as $SiCl_4$

$$SiCl_4 + 4CH_3CH_2OH \rightarrow Si(OCH_2CH_3)_4 + 4HCl \quad (6)$$

compared to that of sodium silicate

$$SiO_2 + 2NaOH \rightarrow Na_2SiO_3 + H_2O \quad (7)$$

Note that hydrolysis of TEOS produces solid silica shells of HSNSs (Figures 2 and 3); therefore, the embodied energy of TEOS will be inherited by HSNSs, indicating that HSNSs with thinner shells, which consume less TEOS, would have lower energy features than those having thicker silica shells. According to eq 5, HSNSs with thinner shells also have lower solid thermal conductivities than those with thicker shells,[23] indicating that improving the thermal performance and lowering the energy feature of HSNSs may be achieved at the same time by controlling the structural parameters of HSNSs. This represents an advantage for achieving superinsulating materials by using hollow nanospheres (Figure 2).

On the basis of the above-mentioned considerations, new synthetic methods that enable HSNSs with low thermal conductivities and low embodied energies can be developed. A $CaCO_3$ nanoparticle templating approach,[67,68] where sodium silicate is used as the silica source material, is under discussion for the preparation of HSNS NIMs.

5. CONCLUSIONS

HSNSs with a typical inner pore diameter of about 150 nm and a shell thickness of 10−15 nm have been prepared by using a PS nanosphere template-assisted approach. The structural features of HSNSs can be controlled by using the PS nanosphere templates with different properties. HSNSs exhibit a reduced thermal conductivity of about 0.02 W/(m K) because of the predominant size-dependent thermal conduction appearing at the nanometer scale. The energy and raw material consumption related to the synthesis of HSNSs has been analyzed by a LCA approach. It is found that HSNSs exhibit a relative high embodied energy, although comparable to that of silica aerogels. Moreover, the LCA results indicate clearly that the recycling of chemicals, up-scaling production, and use of environmentally friendly materials can affect greatly the process environmental footprints of HSNSs. New synthetic approaches can thus be developed to optimize their energy features. More importantly, the methodology reported here can be extended to other nanomaterials, where the concern on their energy and/or environmental impact is of high priority.

In conclusion, HSNS NIMs are comparable to silica aerogels for thermal insulation applications, while exhibiting great flexibility in modifying their properties by tuning the corresponding structural parameters. Further studies dedicated to HSNS NIMs with low thermal conductivities and low embodied energies are therefore interesting and worth pursuing.

AUTHOR INFORMATION

Corresponding Author

*E-mail: tao.gao@ntnu.no.

Notes

The authors declare no competing financial interest.

ACKNOWLEDGMENTS

We thank Dr. A. A. M. Houlihan Wiberg and R. D. Schlanbusch for their helpful discussions. This work has been supported by the Research Council of Norway and several partners through the NTNU and SINTEF "Research Centre on Zero Emission Buildings".

REFERENCES

(1) Wilson, M.; Smith, K. K. G.; Simmons, M.; Raguse, B. *Nanotechnology—Basic Science and Emerging Technologies*; Chapman and Hall/CRC: Boca Raton, FL, 2002; pp 232−249.
(2) Garcia-Martinez, J. *Nanotechnology for the Energy Challenge*; Wiley-VCH: Weinheim, Germany, 2010; pp 3−77.
(3) Zhu, W.; Bartos, P. J. M.; Porro, A. *Mater. Struct.* **2004**, *37*, 649−658.
(4) Lee, J.; Mahendra, S.; Alvarez, P. J. J. *ACS Nano* **2010**, *4*, 3580−3590.
(5) Raki, L.; Beaudoin, J.; Alizadeh, R.; Makar, J.; Sato, T. *Materials* **2010**, *3*, 918−942.
(6) Gesser, H. D.; Goswami, P. C. *Chem. Rev.* **1989**, *89*, 765−788.
(7) Hüsing, N.; Schubert, U. *Angew. Chem., Int. Ed.* **1998**, *37*, 22−45.
(8) Pierre, A. C.; Pajonk, G. M. *Chem. Rev.* **2002**, *102*, 4243−4265.
(9) Baetens, R.; Jelle, B. P.; Gustavsen, A. *Energy Buildings* **2011**, *43*, 761−769.
(10) Jensen, K. I.; Schultz, J. M.; Kristiansen, F. H. *J. Non-Cryst. Solids* **2004**, *350*, 351−357.
(11) Thorne-Banda, H.; Miller, T. In *Aerogels Handbook*; Aegerter, M. A., Leventis, N., Koebel, M. M., Eds.; Springer: New York, 2011; pp 847−856.
(12) Leventis, N.; Sotiriou-Leventis, C.; Zhang, G.; Rawashdeh, A. M. M. *Nano Lett.* **2002**, *2*, 957−960.
(13) Meador, M. A. B.; Fabrizzio, E. F.; Ilhan, F.; Dass, A.; Zhang, G.; Vassilaras, P.; Johnston, J. C.; Leventis, N. *Chem. Mater.* **2005**, *17*, 1085−1098.

(14) Nguyen, B. N.; Meador, M. A. B.; Tousley, M. E.; Shonkwiler, B.; McCorkle, L.; Scheiman, D. A.; Palczer, A. *ACS Appl. Mater. Interfaces* **2009**, *1*, 621−630.
(15) Lee, C. J.; Kim, G. S.; Hyun, S. H. *J. Mater. Sci.* **2002**, *37*, 2237−2241.
(16) Shi, F.; Liu, J. X.; Song, K.; Wang, Z. Y. *J. Non-Cryst. Solids* **2010**, *356*, 2241−2246.
(17) Tappan, B. C.; Steiner, S. A., III; Luther, E. P. *Angew. Chem., Int. Ed.* **2010**, *49*, 4544−4565.
(18) Bigall, N. C.; Herrmann, A. K.; Vogel, M.; Rose, M.; Simon, P.; Carrillo-Cabrera, W.; Dorfs, D.; Kaskel, S.; Gaponik, N.; Eychmller, A. *Angew. Chem., Int. Ed.* **2009**, *48*, 9731−9734.
(19) Zou, J.; Liu, J.; Karakoti, A. S.; Kumar, A.; Joung, D.; Li, Q.; Khondaker, S. I.; Seal, S.; Zhai, L. *ACS Nano* **2010**, *4*, 7293−7302.
(20) Xu, Y.; Sheng, K.; Li, C.; Shi, G. *ACS Nano* **2010**, *4*, 4324−4330.
(21) Xu, Z.; Zhang, Y.; Li, P.; Gao, C. *ACS Nano* **2012**, *6*, 7103−7113.
(22) Jelle, B. P.; Gustavsen, A.; Baetens, R. *J. Build. Phys.* **2010**, *34*, 99−123.
(23) Gao, T.; Sandberg, L. I. C.; Jelle, B. P.; Gustavsen, A. In *Fuelling the Future: Advances in Science and Technologies for Energy Generation, Transmission and Storage*; Mendez-Vilas, A. A., Ed.; Brown Walker Press: Boca Raton. FL, 2012; pp 535−539.
(24) Yue, Q.; Li, Y.; Kong, M.; Huang, J.; Zhao, X.; Liu, J.; Williford, R. E. *J. Mater. Chem.* **2011**, *21*, 12041−12046.
(25) Liao, Y.; Wu, X.; Liu, H.; Chen, Y. *Thermochim. Acta* **2011**, *526*, 178−184.
(26) Kates, R. W.; Clark, W. C.; Corell, R.; Hall, J. M.; Jaeger, C. C.; Lowe, I.; McCarthy, J. J.; Schellnhuber, H. J.; Bolin, B.; Dickson, N. M.; et al. *Science* **2001**, *292*, 641−642.
(27) Savolainen, K.; Alenius, H.; Norppa, H.; Pylkkänen, L.; Tuomi, T.; Kasper, G. *Toxicology* **2010**, *269*, 92−104.
(28) Mueller, N. C.; Nowack, B. *Environ. Sci. Technol.* **2008**, *42*, 4447−4453.
(29) Hischier, R.; Walser, T. *Sci. Total Environ.* **2012**, *425*, 271−282.
(30) Dowson, M.; Grogan, M.; Birks, T.; Harrison, D.; Craig, S. *Appl. Energy* **2012**, *97*, 396−404.
(31) Dahlben, L. J.; Isaacs, J. A. In *Environmental Issues and Waste Management Technologies in the Materials and Nuclear Industries XII*; Cozzi, A., Ohji, T., Eds.; Wiley: Hoboken, NJ, 2009; pp 243−253.
(32) Healy, M. L.; Dahlben, L. J.; Isaacs, J. A. *J. Ind. Ecol.* **2008**, *12*, 376−393.
(33) Singh, A.; Lou, H. H.; Pike, R. W.; Agboola, A.; Li, X.; Hopper, J. R.; Yaws, C. L. *Am. J. Environ. Sci.* **2008**, *4*, 522−534.
(34) Khanna, V.; Bakshi, B. R.; Lee, L. J. *J. Ind. Ecol.* **2008**, *12*, 394−410.
(35) Khanna, V.; Bakshi, B. R. *Environ. Sci. Technol.* **2009**, *43*, 2078−2084.
(36) Walser, T.; Demou, E.; Lang, D. J.; Hellweg, S. *Environ. Sci. Technol.* **2011**, *45*, 4570−4578.
(37) Meyer, D. E.; Curran, M. A.; Gonzalez, M. A. *Environ. Sci. Technol.* **2009**, *43*, 1256−1263.
(38) Krishnan, N.; Boyd, S.; Somani, A.; Raoux, S.; Clark, D.; Dornfeld, D. *Environ. Sci. Technol.* **2008**, *42*, 3069−3075.
(39) Roes, A. L.; Marsili, E.; Nieuwlaar, E.; Patel, M. K. *J. Polym. Environ.* **2007**, *15*, 212−226.
(40) Reijnders, L. *J. Cleaner Prod.* **2010**, *18*, 307−312.
(41) Haynes, W. M.; Lide, D. R. *CRC Handbook of Chemistry and Physics*, 91st ed.; CRC Press: Boca Raton, FL, 2010; Section 6.
(42) Cahill, D. G.; Ford, W. K.; Goodson, K. E.; Mahan, G. D.; Majumdar, A.; Maris, H. J.; Merlin, R.; Philipot, S. R. *J. Appl. Phys.* **2003**, *93*, 793−818.
(43) Heino, P.; Ristolainen, E. *Phys. Scr.* **2004**, *T114*, 171−174.
(44) Zhu, Y. F.; Shi, J. L.; Shen, W. H.; Dong, X. P.; Feng, J. W.; Ruan, M. L.; Li, Y. S. *Angew. Chem., Int. Ed.* **2005**, *44*, 5083−5087.
(45) Du, Y.; Luna, L. E.; Tan, W. S.; Rubner, M. F.; Cohen, R. E. *ACS Nano* **2010**, *4*, 4308−4316.
(46) Jin, P.; Chen, Q. W.; Hao, L. Q.; Tian, R. F.; Zhang, L. X.; Wang, L. *J. Phys. Chem. B* **2004**, *108*, 6311−6314.
(47) Hu, J.; Chen, M.; Fang, X.; Wu, L. *Chem. Soc. Rev.* **2011**, *40*, 5472−5491.
(48) Zhang, T.; Ge, J.; Hu, Y.; Zhang, Q.; Aloni, S.; Yin, Y. *Angew. Chem., Int. Ed.* **2008**, *47*, 5806−5811.
(49) Zhang, T.; Zhang, Q.; Ge, J.; Goebl, J.; Sun, M.; Yan, Y.; Liu, Y. S.; Chang, C.; Guo, J.; Yin, Y. *J. Phys. Chem. C* **2009**, *113*, 3168−3175.
(50) Yu, Q.; Wang, P.; Hu, S.; Hui, J.; Zhuang, J.; Wang, X. *Langmuir* **2011**, *27*, 7185−7191.
(51) Guerrero-Martínez, A.; Pérez-Juste, J.; Liz-Marzán, L. M. *Adv. Mater.* **2010**, *22*, 1182−1195.
(52) Wan, Y.; Yu, S. H. *J. Phys. Chem. C* **2008**, *112*, 3641−3647.
(53) Yang, J.; Lind, J. U.; Trogler, W. C. *Chem. Mater.* **2008**, *20*, 2875−2877.
(54) Du, X.; He, J. *J. Appl. Polym. Sci.* **2008**, *108*, 1755−1760.
(55) Zou, H.; Wu, S.; Ran, Q.; Shen, J. *J. Phys. Chem. C* **2008**, *112*, 11623−11629.
(56) Chen, M.; Wu, L. M.; Zhou, S. X.; You, B. *Adv. Mater.* **2006**, *18*, 801−806.
(57) Cao, S. S.; Jin, X.; Yuan, X. H.; Wu, W. W.; Hu, J.; Sheng, W. C. *J. Polym. Sci., Part A: Polym. Chem.* **2010**, *48*, 1332−1338.
(58) Stöber, W.; Fink, A.; Bohn, E. *J. Colloid Interface Sci.* **1968**, *26*, 62−69.
(59) Liang, L.; Li, B. *Phys. Rev. B* **2006**, *73*, 153303.
(60) Gustafsson, S. E. *Rev. Sci. Instrum.* **1991**, *62*, 797−804.
(61) Liu, L.; Chen, X. *J. Appl. Phys.* **2010**, *107*, 033501.
(62) Teja, A. S.; Beck, M. P.; Yuan, Y.; Warrier, P. *J. Appl. Phys.* **2010**, *107*, 114319.
(63) Desai, T. G. *Appl. Phys. Lett.* **2011**, *98*, 193107.
(64) Bribián, I. Z.; Capilla, A. V.; Usón, A. A. *Build. Environ.* **2011**, *46*, 1133−1140.
(65) Lorenz, D.; Morris, D. *How Much Energy Does It Take to Make a Gallon of Ethanol?*; Institute for Local Self-Reliance: Washington, DC, 1995; pp 1−10.
(66) Bhat, M. G.; English, B. C.; Turhollow, A. F.; Nyangito, H. O. *Energy in Synthetic Fertilizers and Pesticides: Revisited*; Oak Ridge National Laboratory: Oak Ridge, TN, 1994; pp 1−43.
(67) Chen, J. F.; Ding, H. M.; Wang, J. X.; Shao, L. *Biomaterials* **2004**, *25*, 723−727.
(68) Ma, H.; Zhou, J.; Caruntu, D.; Yu, M. H.; Chen, J. F.; O'Connor, C. J.; Zhou, W. L. *J. Appl. Phys.* **2008**, *103*, 07A320.